

***** Chapter 3 *****

Results

The result of the present work are based on the extensive air shower (EAS) data collected using North Bengal University (NBU) EAS array. The studies of EAS detected by using NBU EAS array since 1980 have yielded results on the UHE nuclear interactions and on the composition of primary cosmic rays at the energy range 10^{14} eV to 10^{16} eV. The search for UHE discrete point sources is now the thrust of the NBU EAS project. At the first phase of investigation in this direction a sample of nearly 15,000 events ^{is} taken for the present analysis which were collected by the array during the period Jan 1993 to June 1994. The total run time is 752 hours. Before discussing the main results of the present experiment, the array performance is described. If any large systematic biases involves in the measurement of the air shower observable it will surely reflect on the general characteristics of the observed air showers. The general characteristics of air showers have been studied for a long time and are quite well known. So to make sure that there is no systematic errors in the final results, the general characteristics of the air showers are studied first.

3.1. General Characteristics of the observed EAS :

The results of the present experiment are mainly derived from the density information of the electron component and the muon component of air shower and from the timing information of the shower front.

1. Particle Density data :

One of the main characteristics of EAS is certainly the lateral distribution of the electrons of the EAS. The basic shower parameters for each shower event are estimated in the usual way by fitting the NKG function for the lateral distribution of electrons to the observed densities of the particles. To check the quality of the density information the lateral distribution of electrons is studied. To construct the average lateral distributions the whole radial range is divided into small distance bins. The contribution of electron densities in the different radial distance (from the EAS core) bins for a small bin of shower size and shower age are calculated. The observed lateral distributions of electrons are shown in fig 3.1 and in fig 3.2 for two different shower sizes and shower age along with the NKG distribution curve. It is clear from the fig 3.1 and 3.2 that the

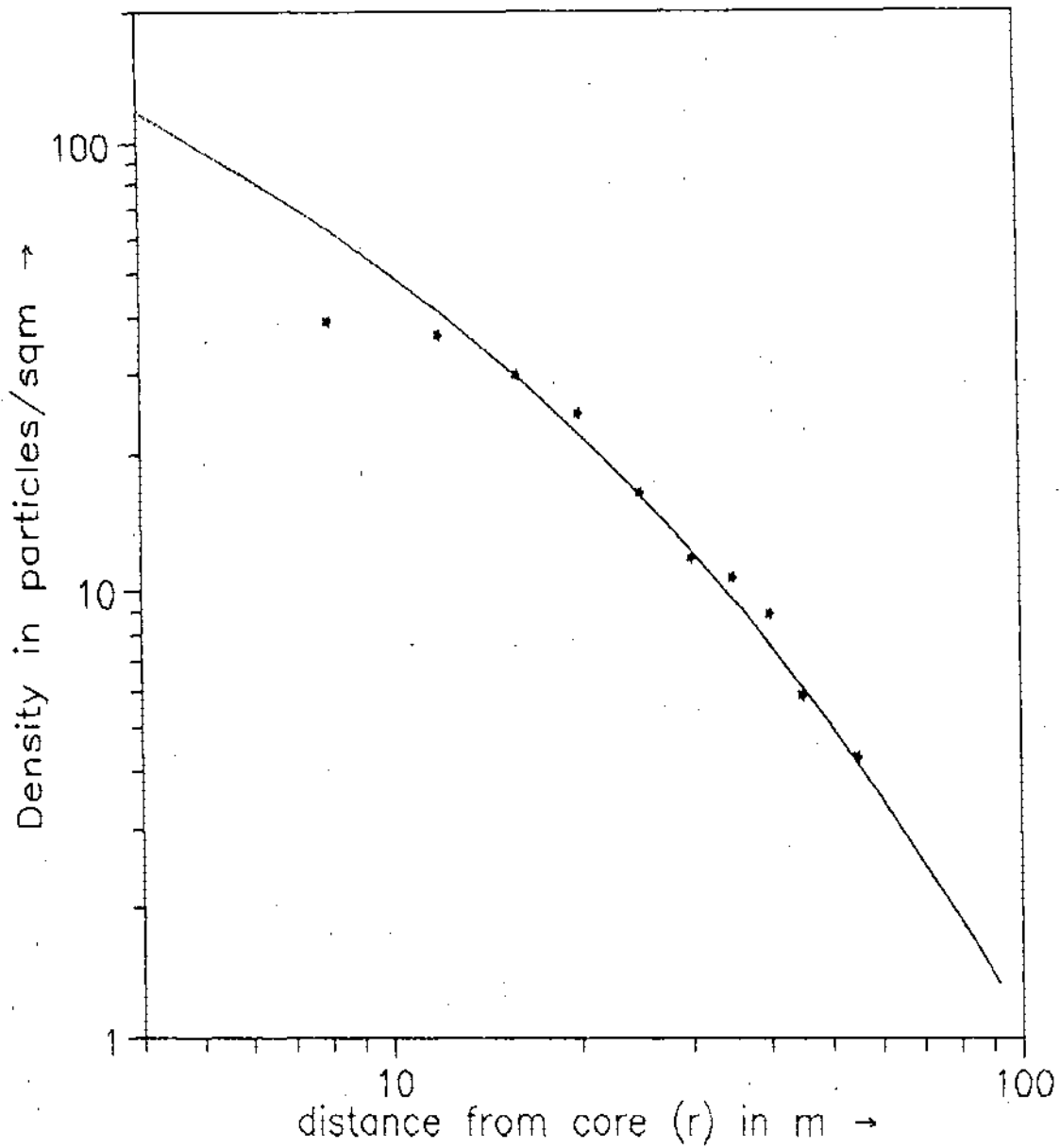


Fig 3.1 Observed radial distribution of the EAS electrons for shower size 2.5×10^5 and for shower age 1.3 compared with the NKG function (solid curve).

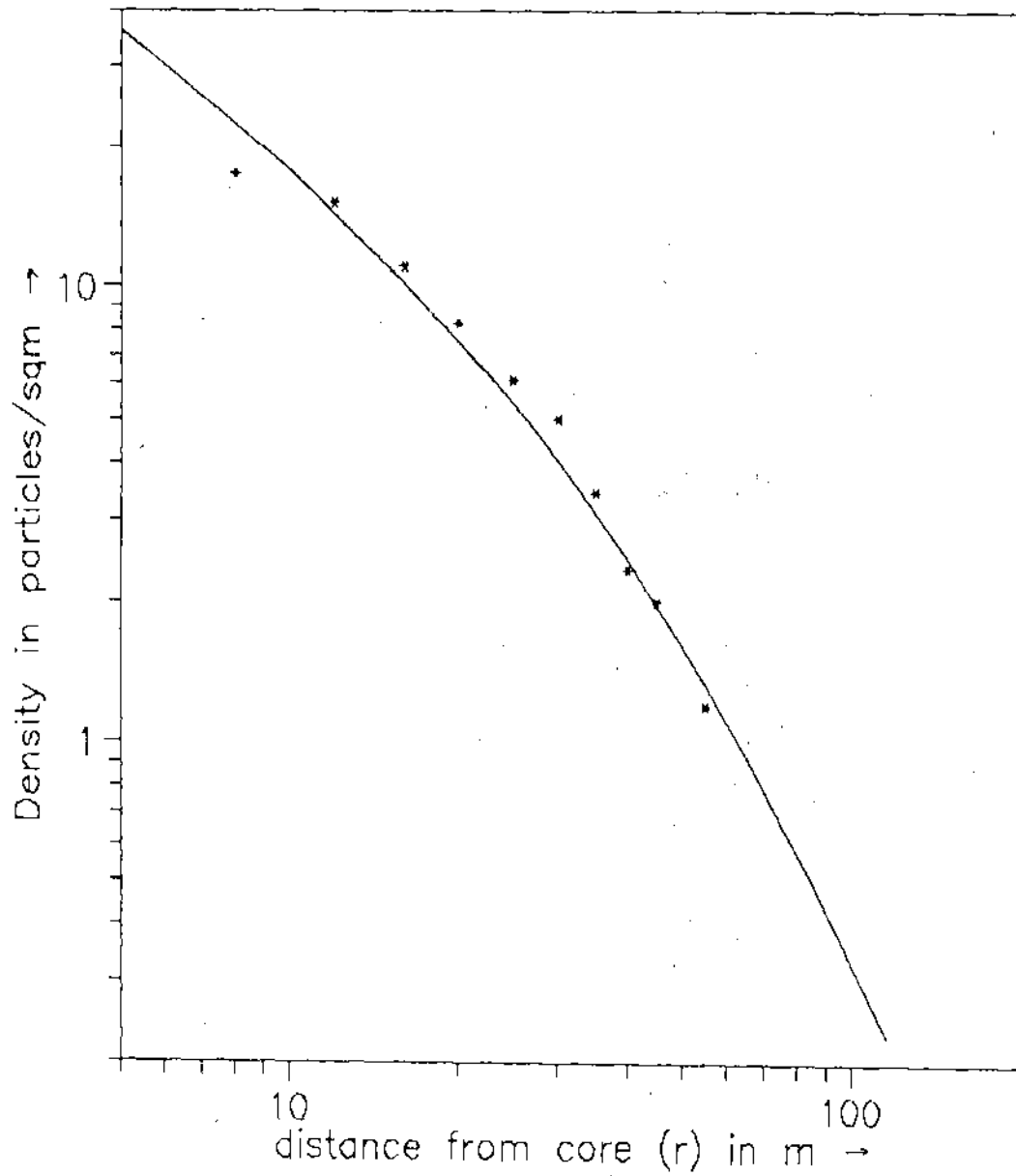


Fig 3.2 Observed radial distribution of the EAS electrons for shower size 8×10^4 and for shower age 1.25 compared with the NKG function(solid curve).

experimental data are in a satisfactory agreement with the NKG function.

The shower 'age' (s) determined by the lateral distribution of shower particles is an important parameter to indicate the stage of longitudinal development. In the fig 3.3 the age distribution obtained from the data is given. The mean 'age' of the observed showers is 1.31 which agrees well with the theoretical estimate (1.33) of Fermyves (1) . The spread of the age distribution is 0.28. The shower size distribution of the observed showers is given in fig 3.4. Showers are detected in the shower size range $2 \times 10^4 - 7 \times 10^6$. The median shower size range detected by the array is $2.4 \times 10^5 - 4.8 \times 10^5$.

2. Muon data :

Muon component of EAS provides very important information regarding the high energy interaction characteristics and about the properties of primaries. Because of the lack of interaction of muons with air nuclei muon component of EAS gives information on shower behavior at the early stage of their development. Total number of muons in an EAS is considered as good measure of the primary energy. A study on muon component of air showers in correlation with other components of the EAS can yield information about the nature of the high energy interactions. The muon size in a shower is estimated by fitting the observed muon density data to a appropriate lateral distribution function. So the lateral distribution of muons in EAS is certainly an important characteristic of EAS.

A representative example of the observed lateral distribution of muons is shown in fig 3.5 for a muon threshold energy 2.5 GeV. The observed densities are fitted with Griesen (2) function given by

$$\rho_{\mu}(r, N_{\mu}, > E_{\mu}) = \Gamma(2.5) / (2 \pi \Gamma(1.25) \Gamma(1.25)) N_{\mu} / r_0^2 (r/r_0)^{-7.5} (1 + r/r_0)^{2.5} \quad \dots 3.1$$

where N_{μ} is the total number of muons in a shower, r_0 is a constant estimated from the fitting which changes slightly with the change of shower size. For $N_e = 2.5 \times 10^5$, r_0 is found to be 290. In the shower size range $10^5 - 10^9$ and for E_{μ} up to 500 GeV Greisen (3) proposed a lateral distribution

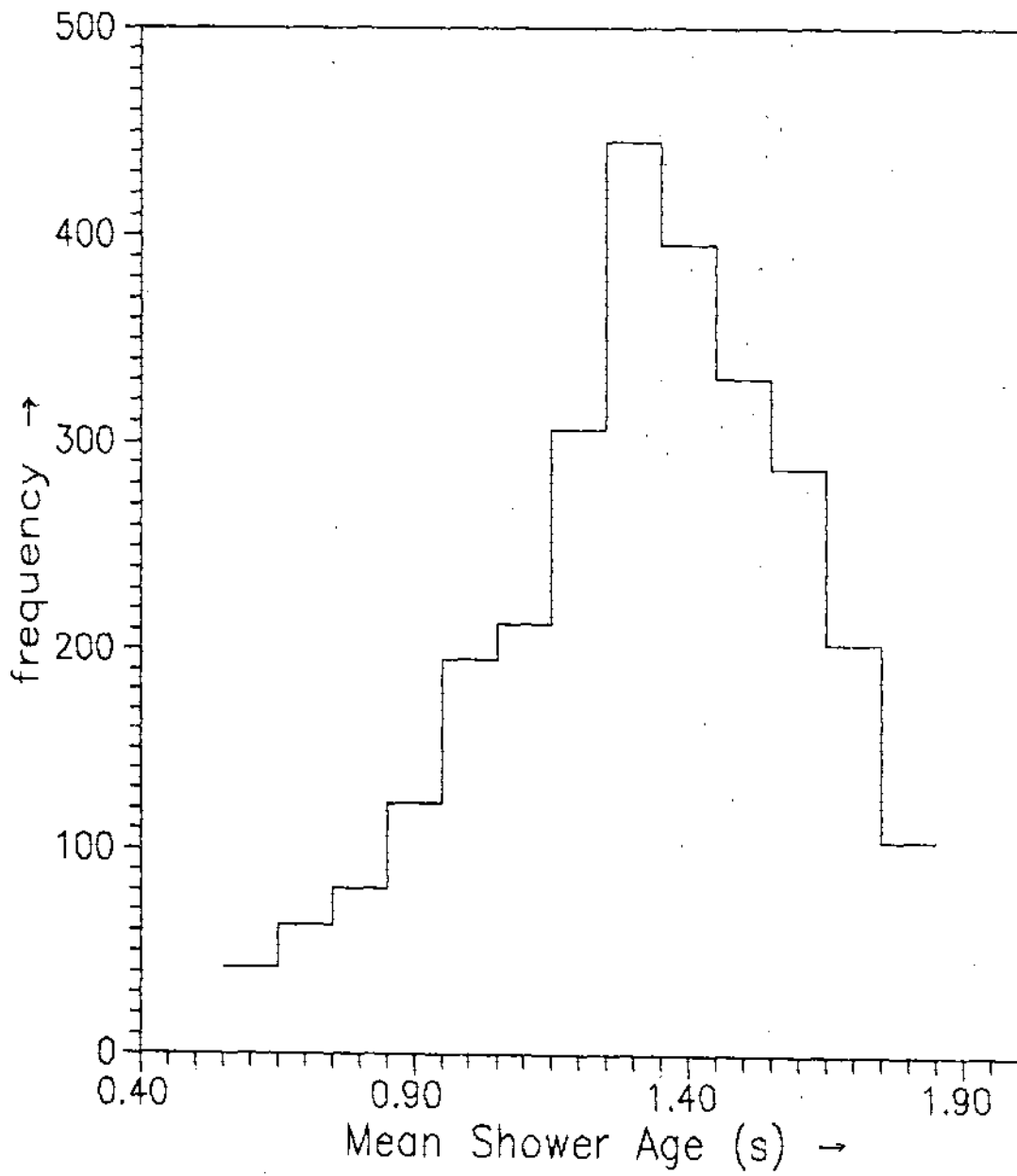


Fig 3.3 Shower age distribution for the observed shower events

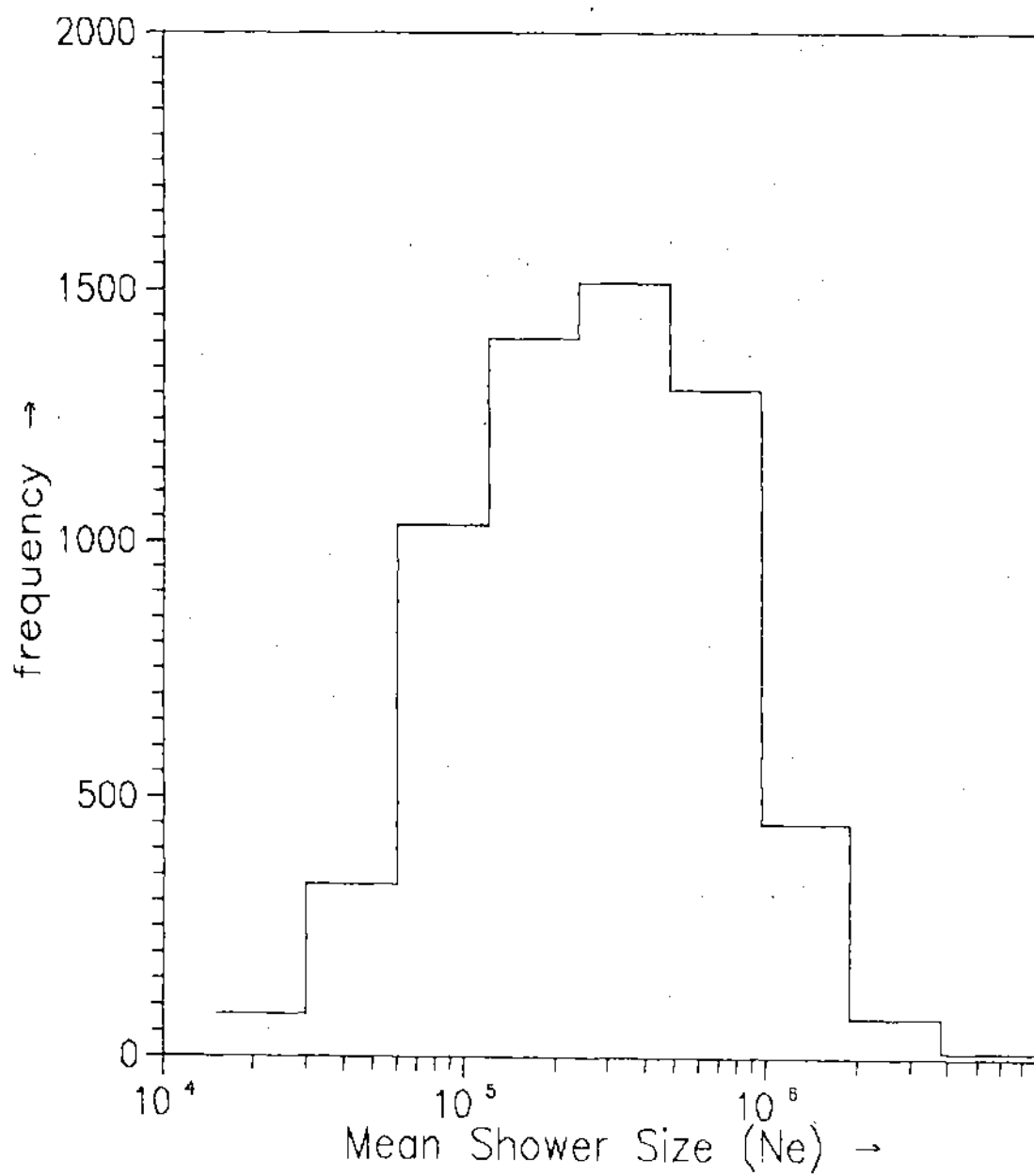


Fig 3.4 Shower size distribution for the observed air showers

formula for muons which is given by

$$\rho_{\mu}(r, N_g, > E_{\mu}) = (N_g/10^6) (14.4 r^{-0.75}) (1 + r/320)^{-2.5} (51/(50 + E_{\mu})) (3/(E_{\mu} + 2))^{0.14r} \dots 3.2$$

A dashed curve in the fig 3.5 represents the Griesen formula. The observed distribution is agreed well with the Griesen formula.

3. Timing information of the shower front :

Arrival direction of each EAS event is determined by usual first timing technique as described in the previous chapter. Since the ultra high energy primary cosmic rays are highly isotropic, the azimuth angle distribution of cosmic ray air showers is expected to be uniform. The azimuth angle distribution of the observed showers is given in fig 3.6 which is consistent with the expectation. The zenith angle distribution of the EAS events is also studied to check the array performance. The errors of zenith angle measurements in individual EAS event do not exceed 1.5° . Shower events in the size range $2 \times 10^4 - 5 \times 10^6$ particles for zenith angles from 0° to 60° are considered. The distribution is given in fig 3.7. The zenith angle dependence of the integral flux of showers can be expressed by a power function in the form (2)

$$I(\theta) = I_0 \cos^{\alpha} z \dots 3.2$$

i.e, the flux of showers monotonically decreases with the increase of zenith angle. This is due to atmospheric absorption which increases with zenith angle as the inclined showers traverse an increased thickness of atmosphere. However the number of events observed for a given zenith angle range increases with zenith angle first, reaches a peak at around 20° and then falls. This is because the solid angle of acceptance increases with zenith angle as $\sin(z)$. At higher zenith angles the atmospheric absorption part dominates over the solid angle of acceptance part and as a result the number of events within a zenith angle bin falls. To remove the solid angle effect the frequency of events are divided by $\sin(z)$ and plotted against $\cos(z)$ which is shown in fig 3.8. From the figure the value of the index is found to be 7.64.

The declination distribution of the collected showers is shown in fig 3.9. From the distribution it is found that the effective observation region in the sky by the array is within the

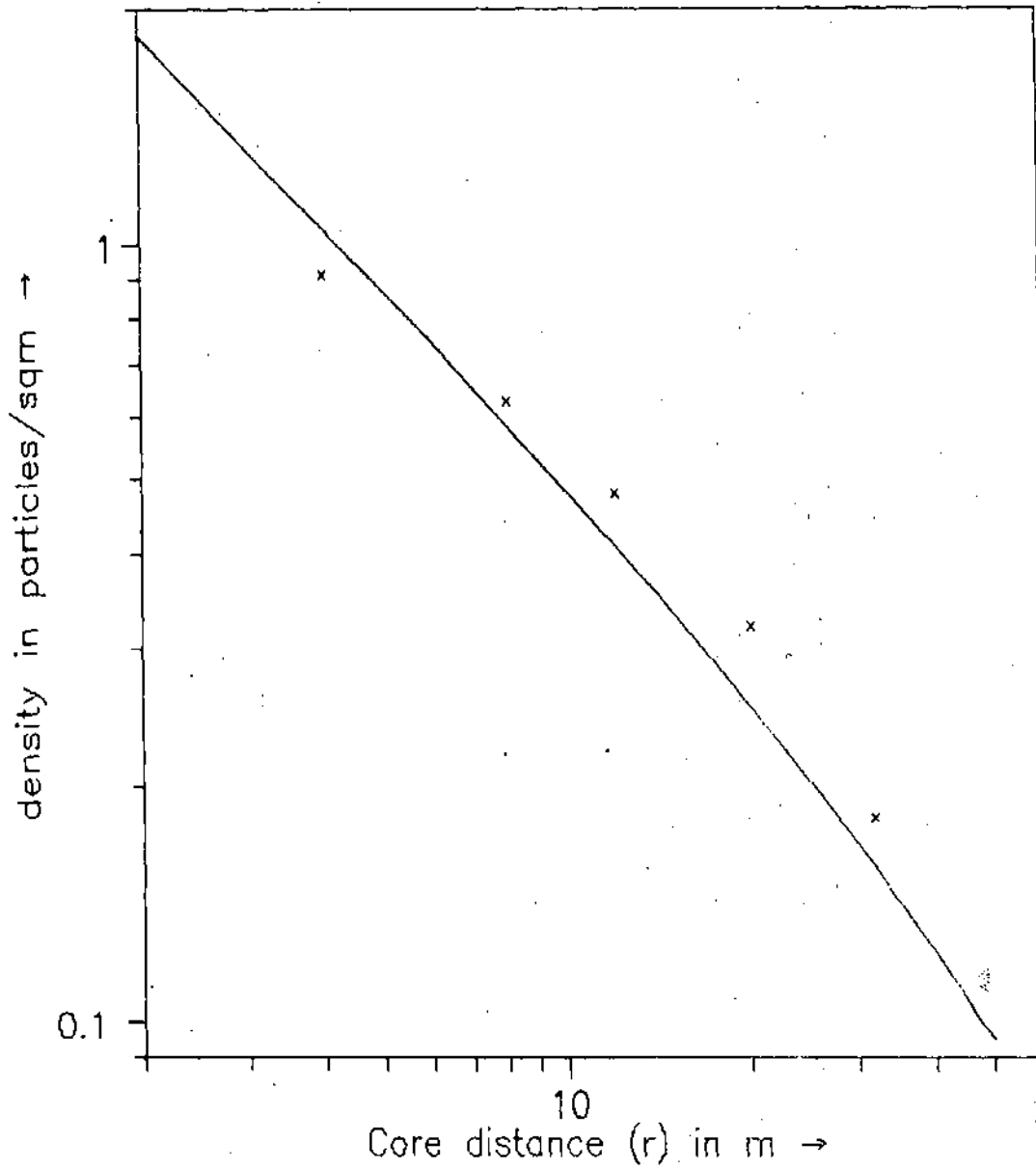


Fig 3.5 Observed radial distribution of EAS muons for the muon threshold energy 2.5 GeV for shower size, $N_e = 2.5 \times 10^5$. The solid curve represents the Greisen formula.

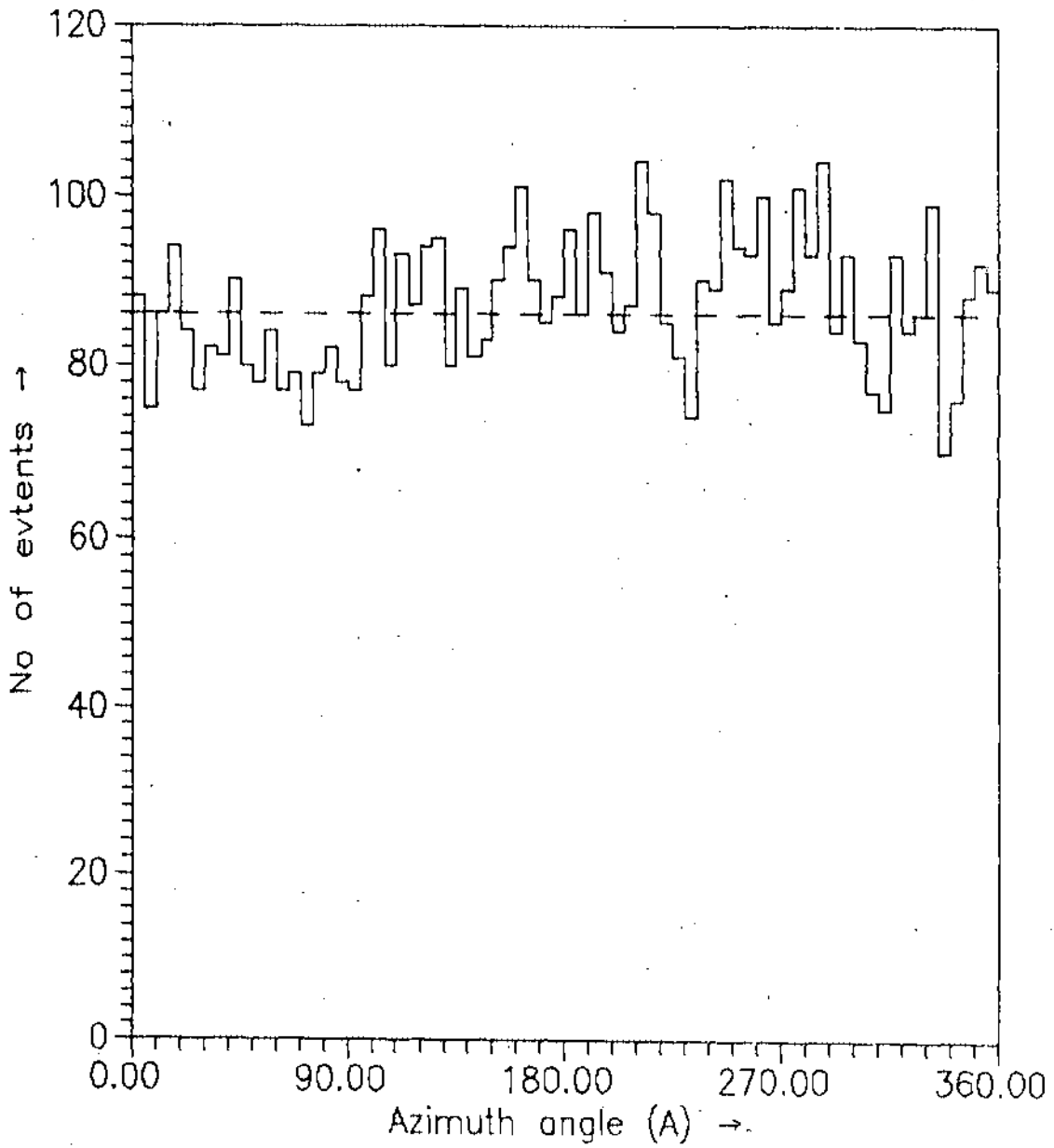


Fig 3.6 Azimuth angle distribution of the observed showers. A dashed line is the average number of showers per bin.

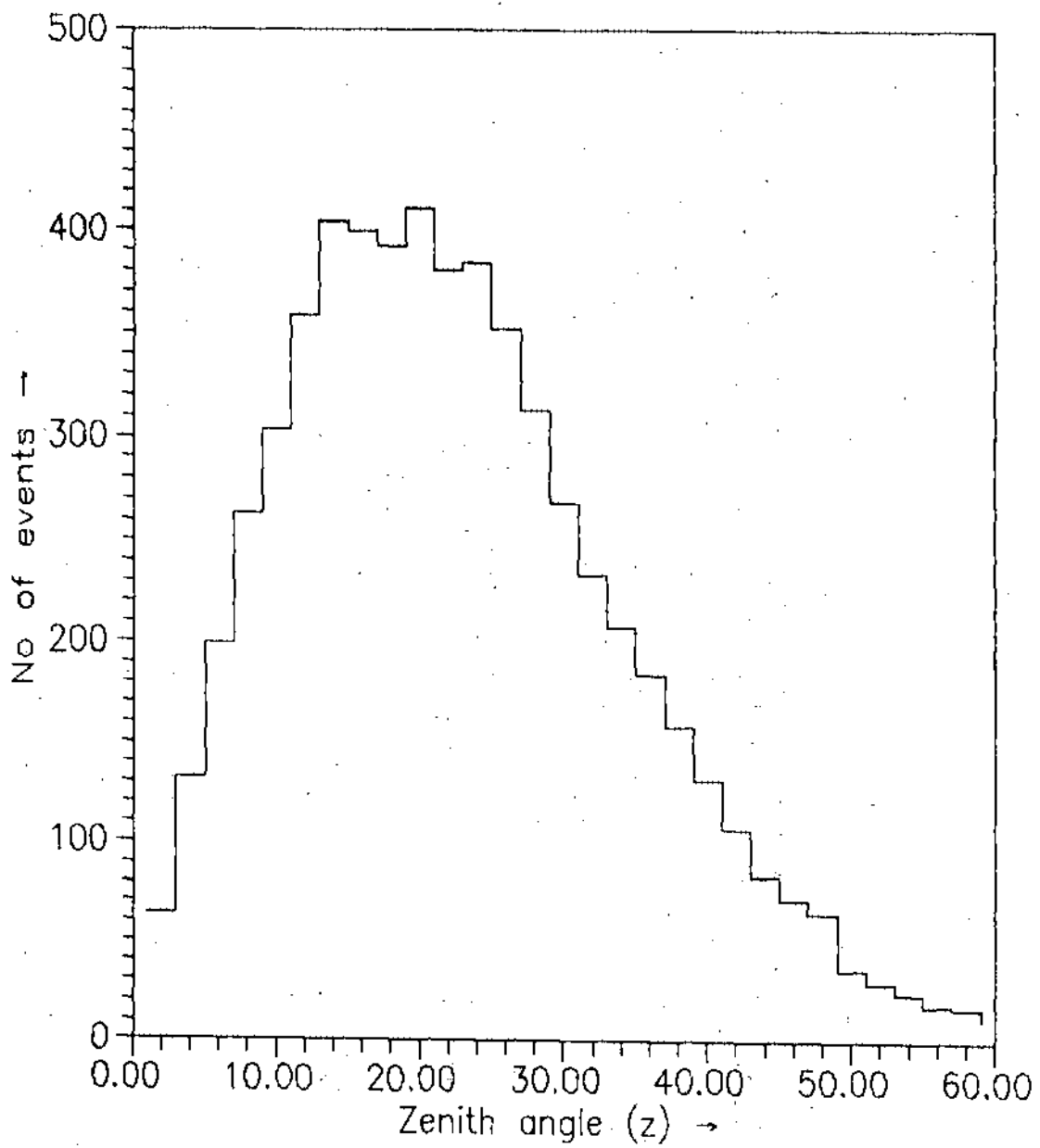


Fig 3.7 Zenith angle distribution of the observed showers

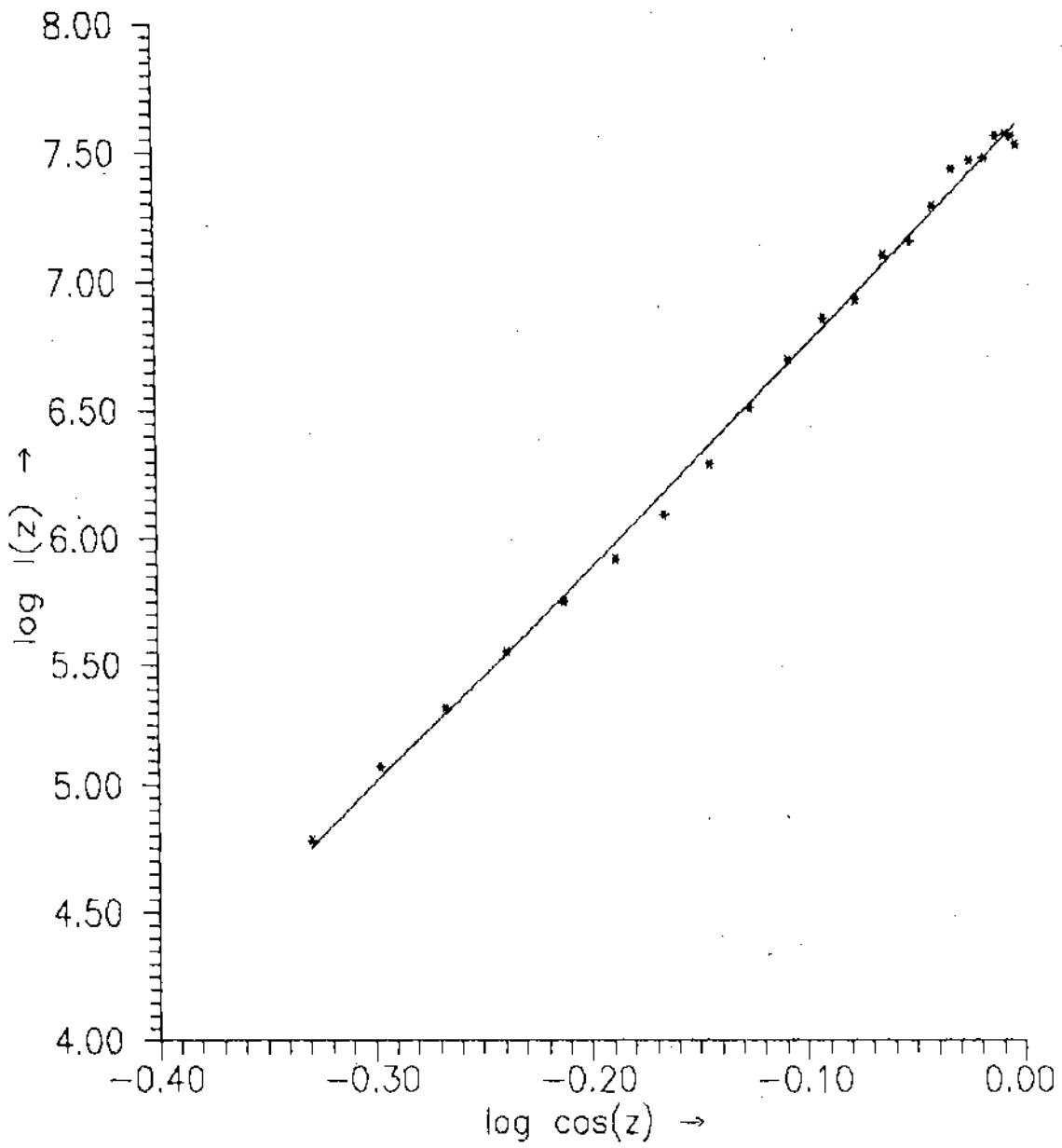


Fig 3.8 Zenith angle dependence of the observed cosmic ray flux.

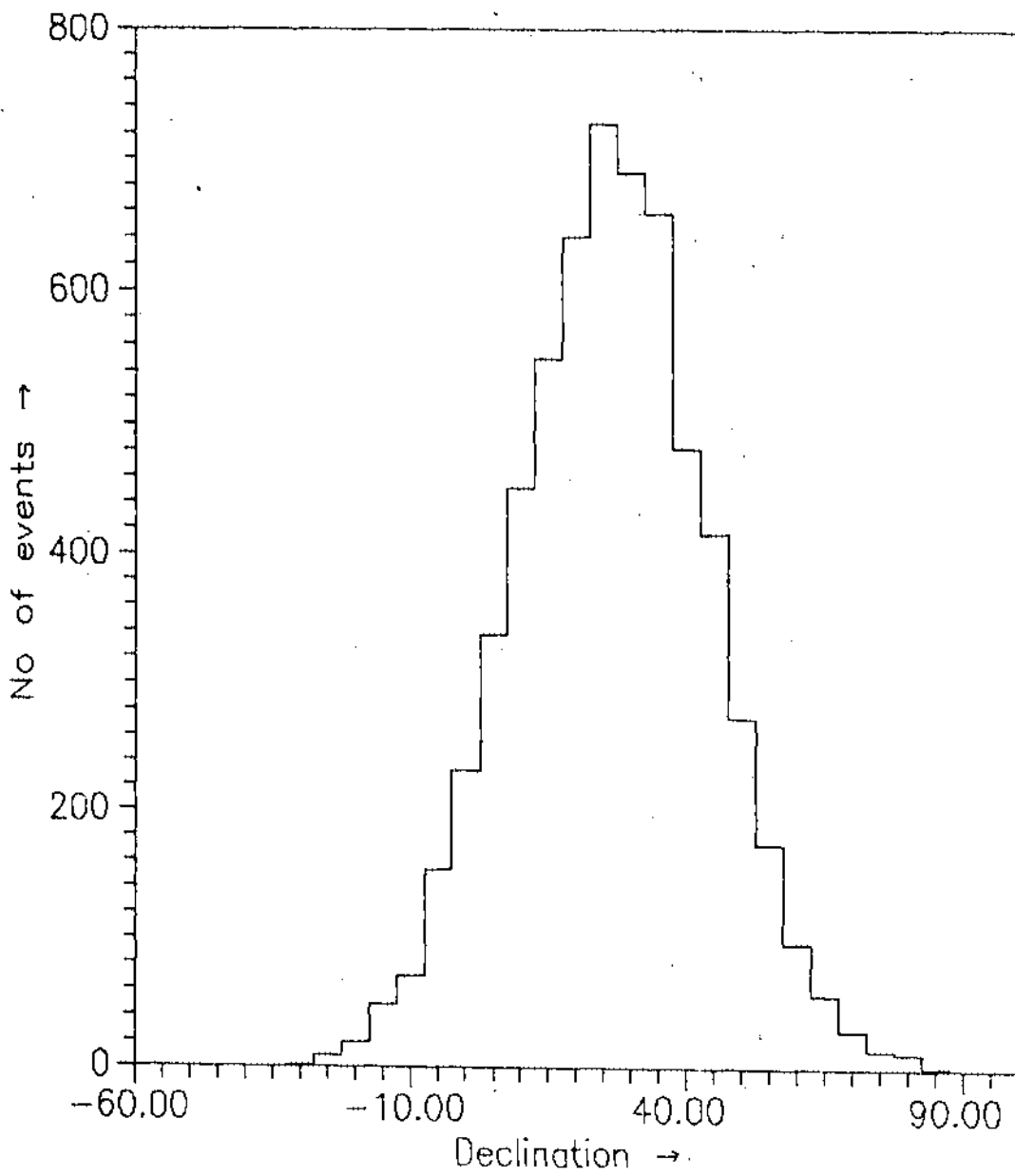


Fig 3.9 Declination distribution of the observed showers

declination range 10° to 50° . It is well known that the most of the potential sources of northern hemisphere like Cygnus X-3, Hercules X-1, Crab Nebula, Geminga fall within this declination range. So the array can observe these sources very effectively.

The isotropic behavior of the cosmic rays should reflect in the right ascension distribution of the observed shower events. A prerequisite of any directional isotropy analysis is that the detector zenith should spend equal times in all right ascension intervals. The equalization of the operating time is implemented by random rejection of the events in each group of hourly intervals in excess of the minimum number for each hour interval. The right ascension distribution obtained using the above procedure for the observed showers is shown in fig 3.10. The distribution is consistent with the isotropic behavior of the UHE cosmic ray particles.

So the general features of the observed air showers are consistent with the well known characteristics of air showers.

3.2. Study on shower parameters :

Muon content in a shower and shower 'age' are the two parameters which are often used to discriminate gamma photon initiated showers from the hadron initiated showers.

1. Study on shower age parameter :

The longitudinal development of EAS is an essential feature that reflects the gross feature of particle interaction at high energies. The stage of development of an air shower is described by shower age parameter (s). The value of s equals to one when the shower is at the stage of maximum development. In the search for UHE gamma ray sources by the EAS method, several workers have made age cut to reduce the EAS background caused by primary cosmic ray charged particles. But the simulation results of Fenyves (1), Hillas (4) and Cheung and Mckeown (5) opposed the idea that the age parameter can be used as a differentiator of gamma ray initiated showers from hadron initiated showers, though it is an observed fact that the age cut produces results.

In most of the observations the showers from point sources were observed at large angles during most of the observation time due to high angle of transit of the sources at the arrays. As for

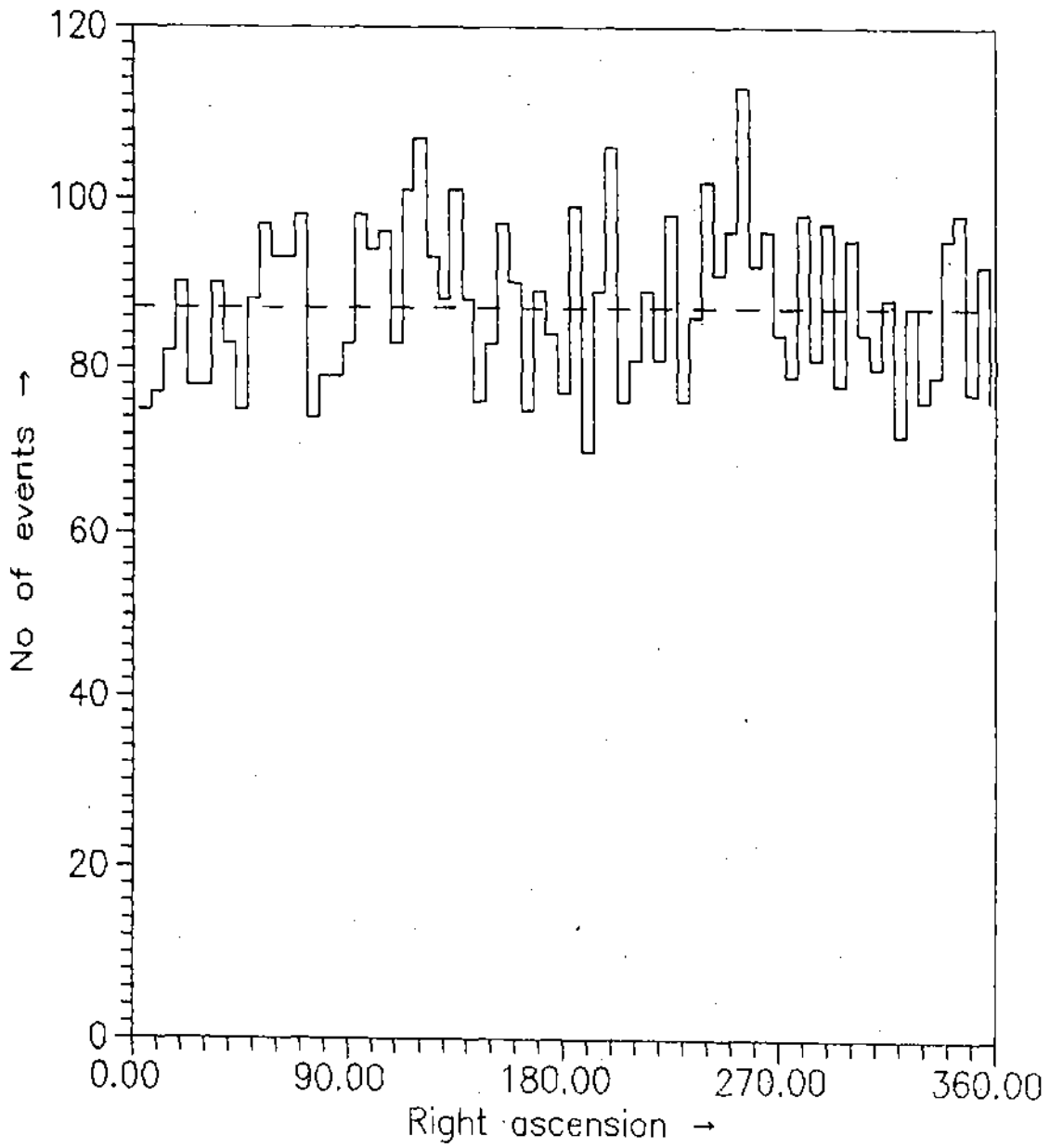


Fig 3.10 Right Ascension distribution of the observed showers. A dashed line corresponds to the average number of showers per bin.

example, Cygnus X-3 is observed at Kiel at zenith about 14° , the same source is observed at Ooty at zenith angle nearly 26° at the transit. Remembering this feature, in the present experiment, the zenith angle dependence of shower 'age' parameter is studied. The variation of mean shower 'age' with zenith angle is shown in fig 3.11 for the whole shower size range ($2 \times 10^4 - 6 \times 10^6$). At the zenith the mean shower 'age' value 1.26. The variation of s with zenith angle (z) is found slow and at $z = 60^\circ$ the mean 'age' reaches only 1.46 though at zenith angle 60° the atmospheric overburden is nearly double. In Buckland park experiment (6) and in Chacaltaya experiment (7) similar trend of variation were observed. Theoretically the variation is much faster.

The total amount of matter in the atmosphere increases in proportion to $\sec z$. The variation of ' s ' with $\sec z$ is also plotted in Fig 3.12. The variation of ' s ' with $\sec z$ can be represented by the linear relationship

$$s(z) = .25 \sec z + 1.05 \quad \dots\dots \quad 3.4$$

The variation of shower age with shower size for the observed showers is shown in fig 3.13. From the figure it is found that the value of average age monotonically decreases with the increase of shower size but the rate of decrease decreases with the increase in the shower size. This is probably due to the variation of effective collection area of the array with the primary energy. Similar trend of variation of shower 'age' with shower size was found in Akeno experiment (8).

2. Study on muon component of EAS :

Results of investigation on muons with energies above 2.5 GeV arriving at the sea level are reported here. The muon component of EAS carry information regarding the high energy interaction characteristics as well as the properties of primary cosmic ray particles. Muon content in a shower is considered as a best parameter to identify gamma ray initiated showers from the hadron initiated showers. It is believed that the gamma ray showers contain less than 10% of muons of normal showers. However in a number of observations it was found that the total muon number in the excess showers from the direction of point sources is almost same as that of normal showers. To better understand the problem in the present investigation the variation of the ratio of the muon density to electron density with shower age for particular core distance at a fixed shower size is studied.

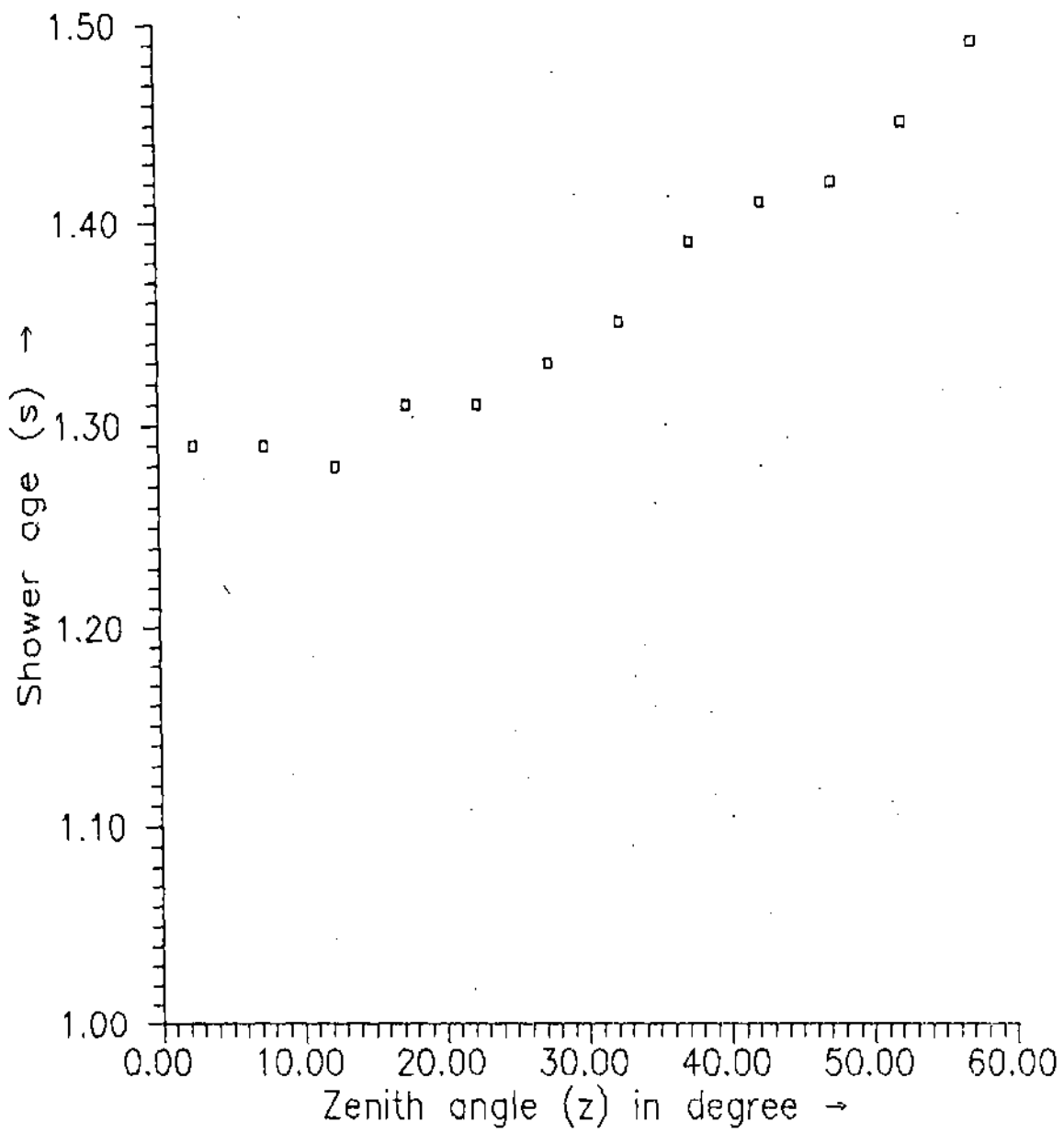


Fig 3.11 Variation of shower age parameter (s) with zenith angle (z) .

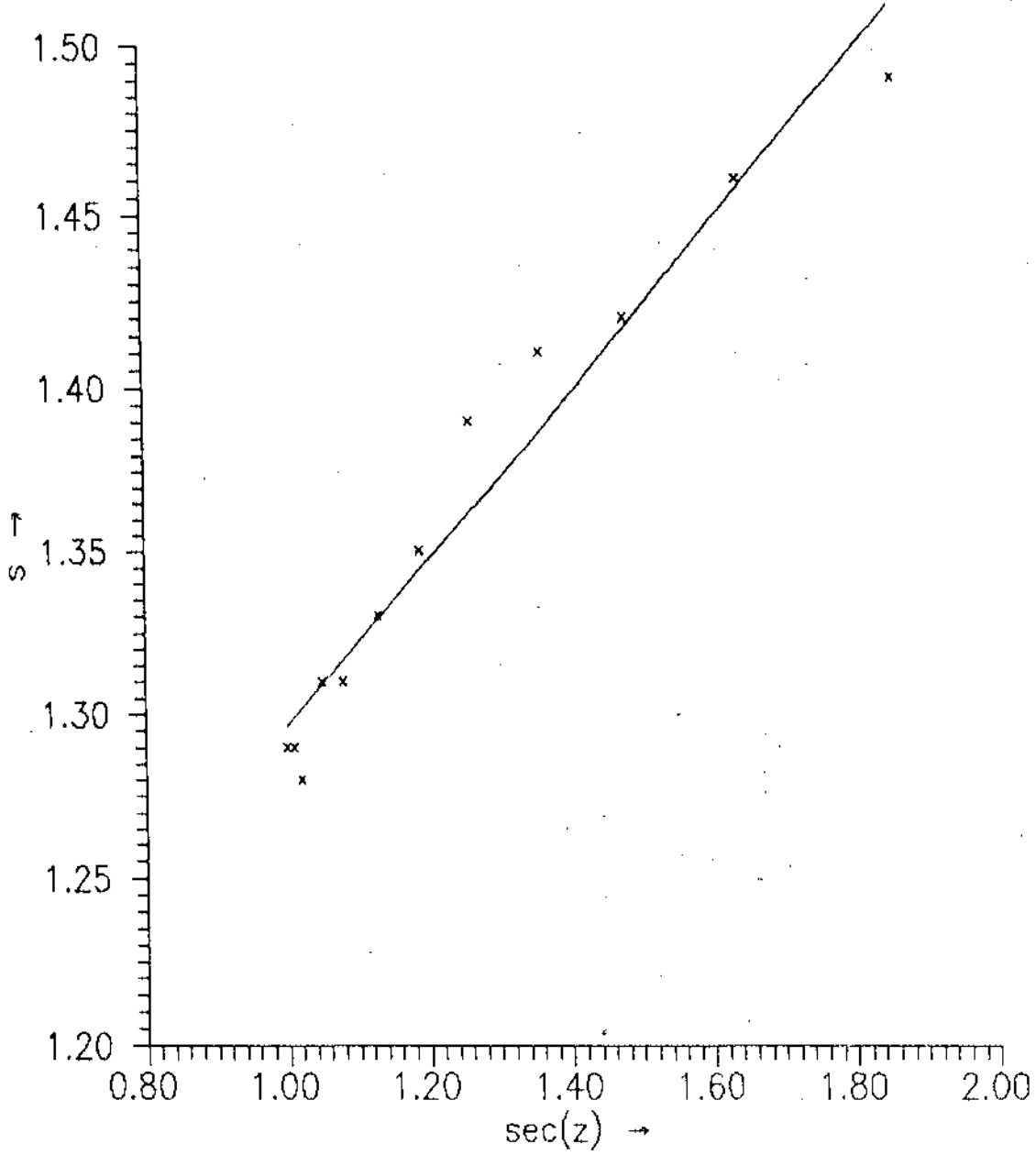


Fig 3.12 Variation of shower age with $\sec(z)$. The solid line is the straight line fitting of the data.

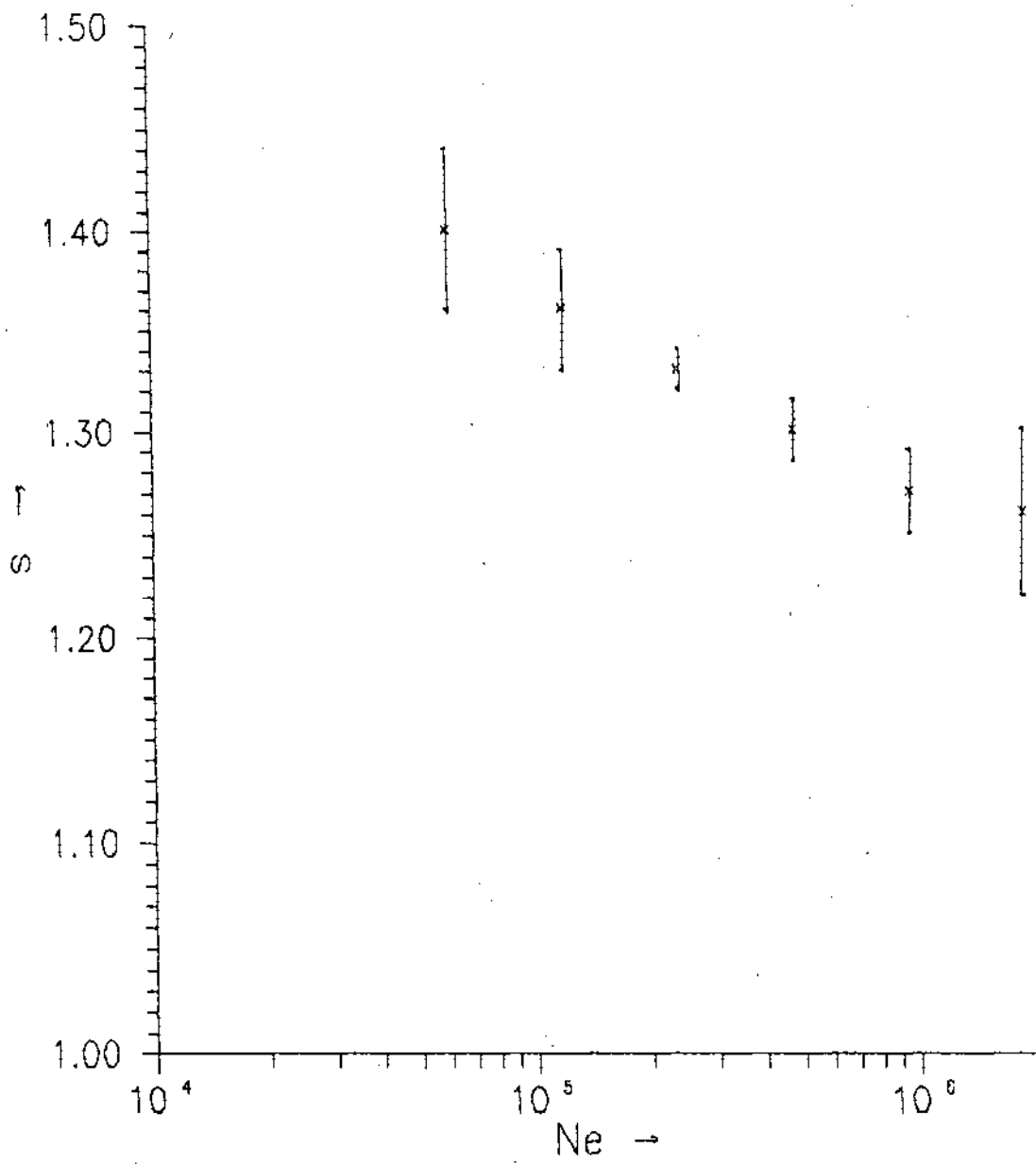


Fig 3.13 Variation of shower age parameter (s) with shower size

The variation of the ratio ρ_μ/ρ_θ with shower age for shower size 2×10^5 at radial distance (from the shower core) 12 m and 20 m are shown in fig 3.14 and 3.15. The radial bins are made wide enough (4m) to accommodate the error in r_μ (~ 2). From the figure it is clear that the ρ_μ/ρ_θ ratio increases as shower age increases. This is expected because the muon number does not change much with the atmospheric depth traversed after the maximum development of shower reaches while shower size decreases rapidly with the increase of shower age. It is interesting to note that high muon content of the excess showers from the direction of Cygnus X-3 as observed by the Kiel group is also characterised by high 'age' values.

The muon size (N_μ) in a shower is obtained using measured lateral distribution of muons fitted to Griesen function

$$\rho_\mu(r, N_e, > E) = \Gamma(2.5) / (2\pi \Gamma(1.25) \Gamma(1.25)) N_\mu / r_0^2 (r/r_0)^{-7.5} (1 + r/r_0)^{-2.5}$$

with the variable r_0 . The variation of muon size with shower size (N_e) is given in fig 3.16. The variation can be represented by a power law relation given by

$$N_\mu = a N_e^\alpha \quad \dots\dots\dots 3.5$$

where a is a constant. The value of the exponent (α) is found to be 0.69. The result is compared with the simulation results of Wrotniak and Yodh (9) for the model F-Y00 for muon threshold energy 2 GeV which is represented by a dashed curve in the fig 3.14. The model assumes mean free paths for the inelastic interactions are energy independent, inelasticity is uniform in (0,1) for nucleons and (1/3,1) for mesons, inclusive distributions in x for secondaries are energy independent (scaling extrapolation of the ISR data) and secondary products are 60% charged pions, 30% neutral pions, 5% charged kaons and 5% neutral kaons. The value of exponent (α) from the said simulation result (.71) is close to the present observation.

3.3. Results of observations for UHE point sources :

The NBU air shower database has been examined for continuous emission of ultra high energy radiation from four potential sources of northern hemisphere, namely, Cygnus X-3, Hercules X-1, Crab-nebula and Geminga. Evidences of any periodic signal with their well known orbital periods from the two sources, Cygnus X-3 and Hercules X-1, are also examined using the

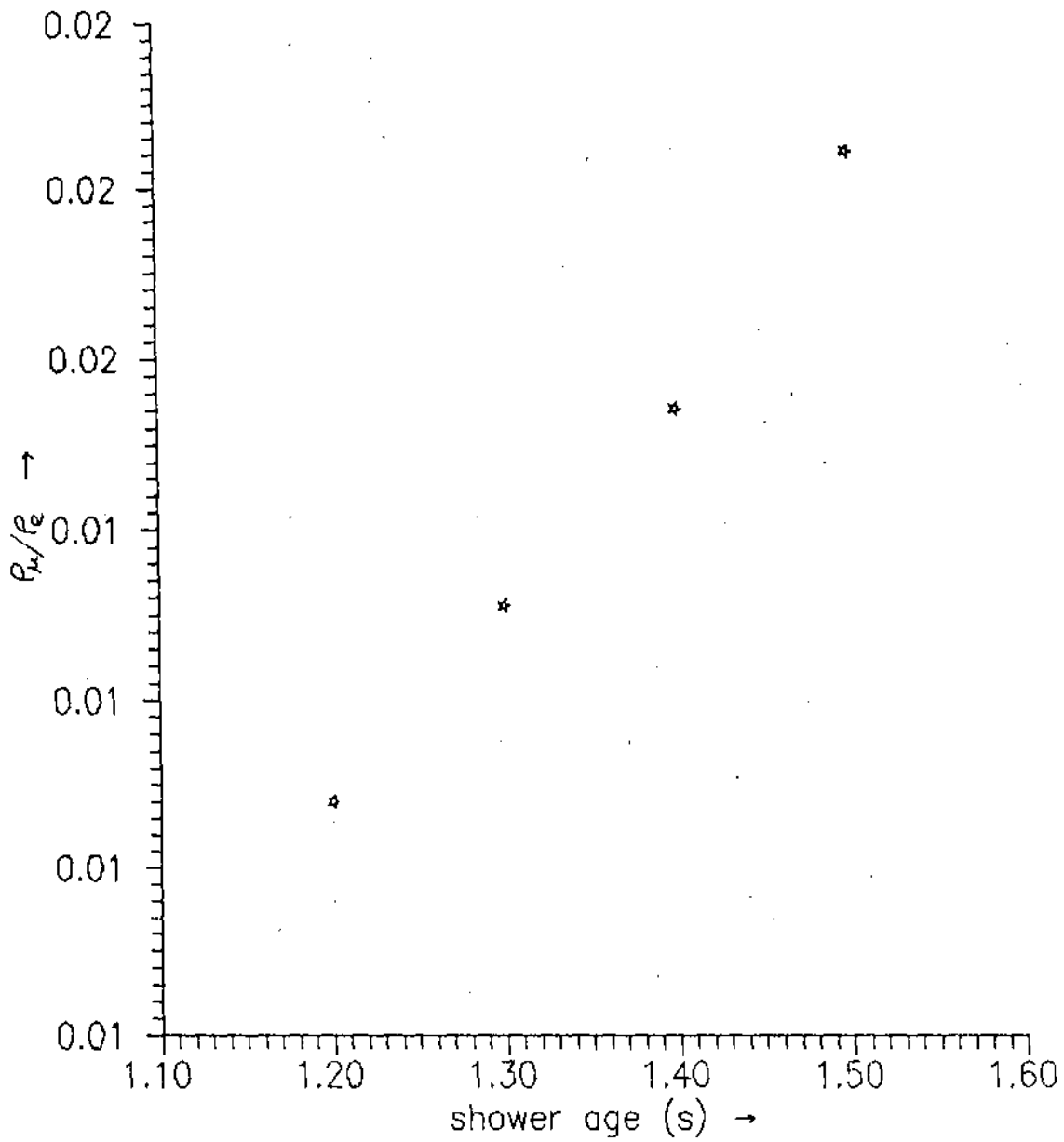


Fig.3.14 Variation of the ratio of muon density to electron density with shower age at core distance 12 m for shower size 2.5×10^5 .

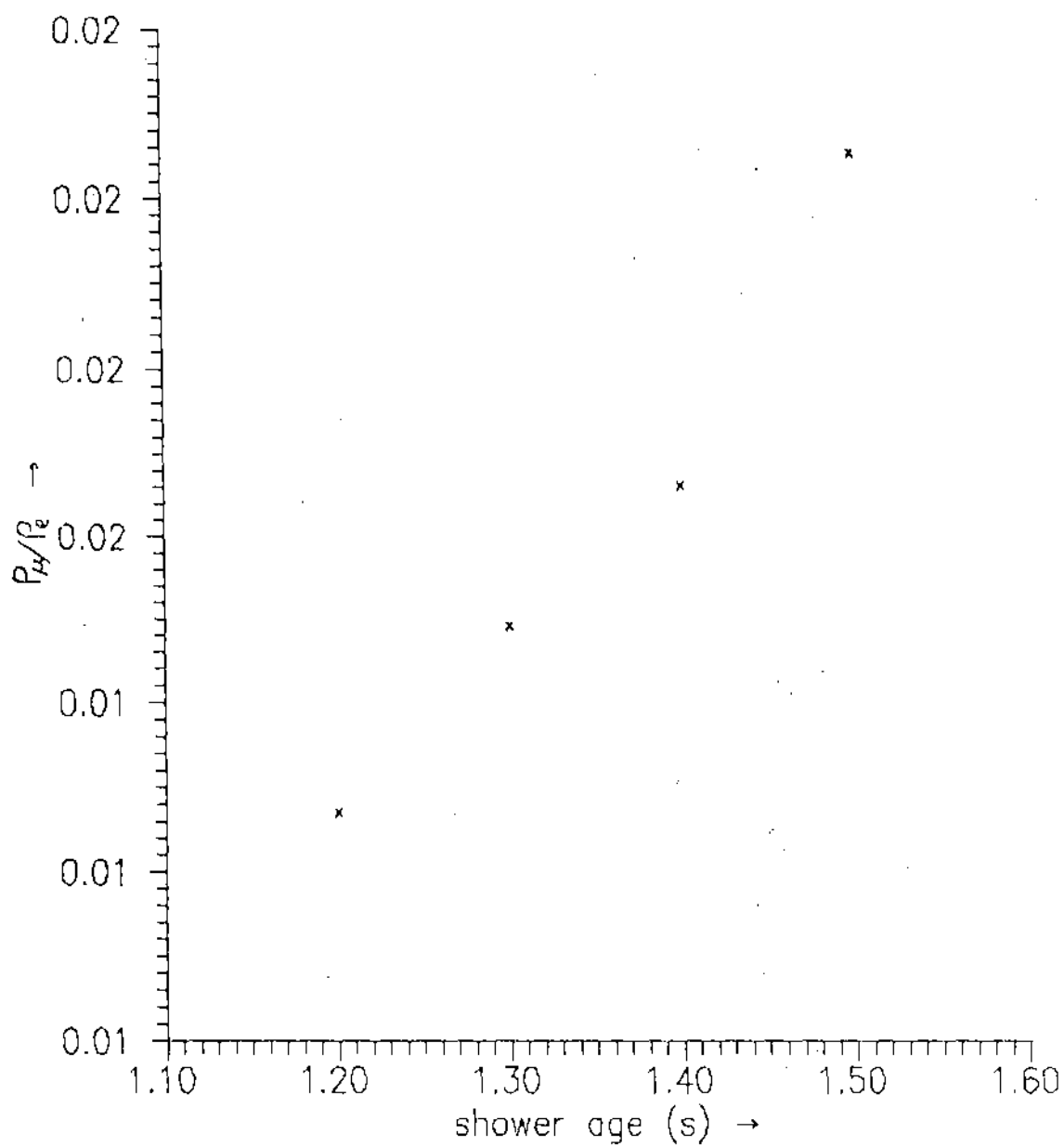


Fig.3.15 Variation of the ratio of muon density to electron density with shower age at core distance 20 m for shower size 2.5×10^5 .

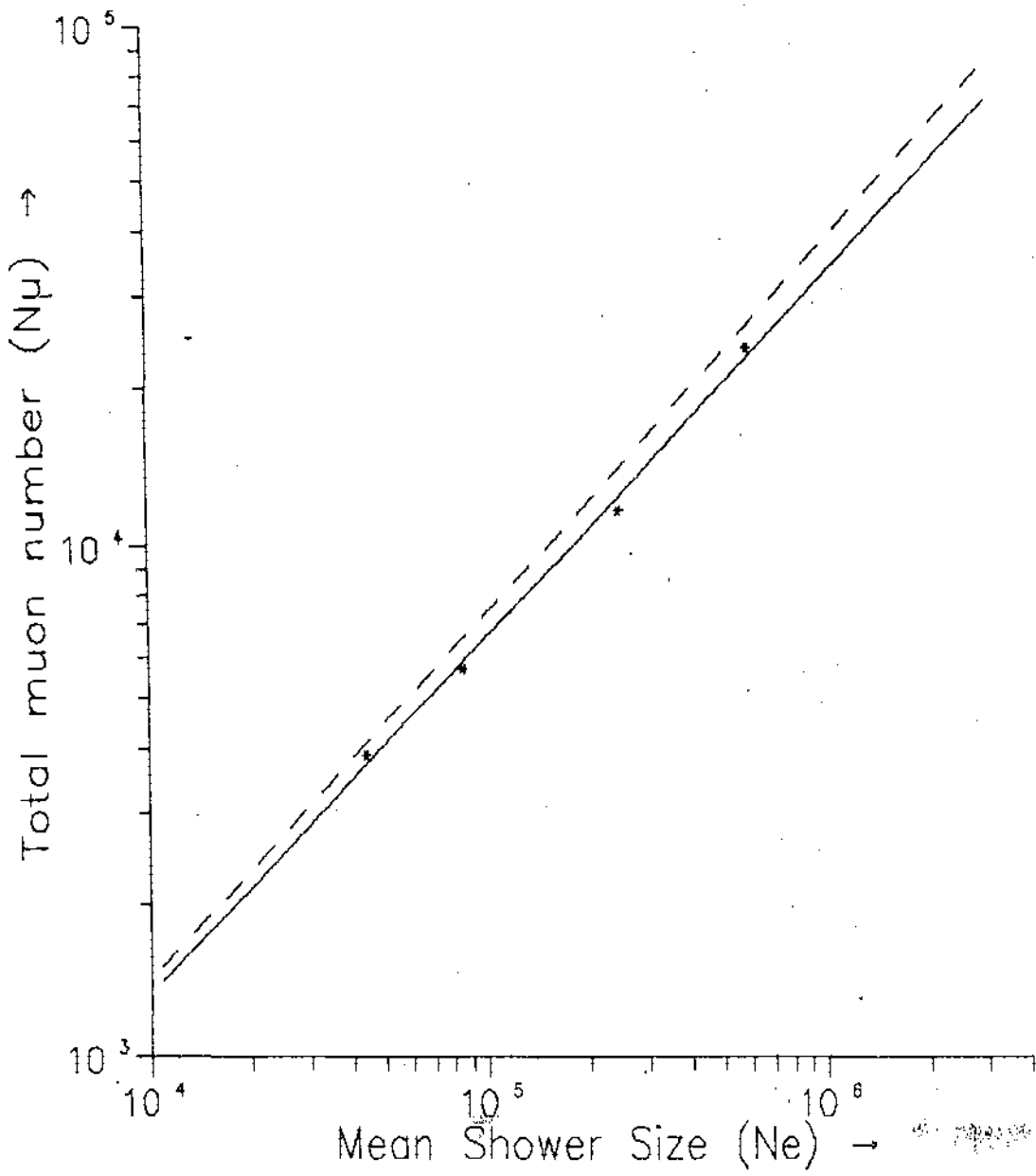


Fig 3.16 Observed muon size dependence on shower size. The dashed line corresponds to simulation results (model F-Y00) of Wrotniak and Yodh(10).

database.

Steady emission of gamma rays from a point source is reflected in an excess of showers from the direction of source compared to the steady flux of charged cosmic ray showers in that direction. In order to examine an excess of showers from a point source, the sky is divided into bins based on equatorial co-ordinates. Signal candidate events are those falling into a square bin of width 5° in declination and width 6° in right ascension. The angular resolution deduced from the odd-even sub-array comparison method is 1.1° in declination and 1.47° in right ascension. But a wider bin is chosen for the search because all the timing counter did not always give timing information. On the average 5.5 timing information was available in a shower event. Approximately 95% of events from the direction of a source are expected to arrive in the source bin. To find out whether an excess really exists in the number of showers from a given direction it is essential to know the steady flux of charged primary initiated cosmic ray showers (background) in that direction quite accurately. The main problem of estimation of the background correctly is the non-uniform exposure of different right ascension-declination region of sky both in sidereal time and in zenith angle. With the time, different right ascension-declination bins drift through different zenith angles and as air showers have a fairly steep zenith angle distribution it is not possible to estimate the background in a straight way. Care has to be taken to ensure that the source and background events are collected during the same time in the same zenith angle intervals. The background is normally evaluated from the number of events in equal sized 'off-source' bins located in the same declination strip as that of source bin but at different right ascensions. In the present analysis the background is determined as follows.

Twelve 'off source' right ascension bins, of equal width as the source bin, in the source declination band six on either side of the source bin are selected. Events are collected for each off source bin in such a way that all the 'off source' bins and the 'on source' bin are exposed for equal time and zenith angle. The average rate of events per bin gives the background count. As the background events are collected from an area twelve times larger than that of source events, the background is determined with good statistical accuracy.

Flux is calculated directly from the on-source time. For this purpose effective area of the array is determined using monte carlo simulation method.

Effective area of the array :

To measure the flux of photon induced showers from a point source, one needs to know the effective area of the air shower array as a function of primary energy and zenith angle. The effective area of an air shower array can be obtained through the Monte Carlo study of the array response. The effective area is calculated by finding how many of the simulated showers meet the array trigger condition. We follow the procedure prescribed by Crewther and Protheroe (10). Shower size is generated using the parameterization given by Crewther and Protheroe (10) for gamma ray initiated showers. Shower age is sampled according to the proposition of Feriyyes et al (11). The number of particles at different radial distances are obtained using NKG function (as the charged particles are expected to follow NKG distribution function). Poisson fluctuation is given to the particle number passing through the detectors. Then each of the simulated showers is checked whether they meet the array trigger requirements or not. A large number of showers is simulated to estimate the effective area of the array. The effective area of the array is plotted against primary gamma ray energy for two different zenith angles and is shown in fig 3.17.

The showers with core falling outside the perimeter of the array are rejected outright. The lowest ~10% of shower sizes are discarded as the angular resolution worsens near the array threshold. The showers with zenith angle less than 45° were only accepted for this analysis. The vertical intensity of the cosmic ray charged particles are calculated first using the effective area obtained from the simulation result. The observed vertical intensity ($I(>8 \times 10^{14} \text{ eV}) = 4.10 \times 10^{-10} \text{ cm}^{-2}\text{sr}^{-1}\text{s}^{-1}$) agrees well with value obtained from the expression ($I(>E) = (E/2)^{-a} \times 10^{-10} \text{ cm}^{-2}\text{sr}^{-1}\text{s}^{-1}$, where E is in PeV and $a = 1.55$ for $E < 2 \text{ PeV}$ and $a = 2.1$ for $E > 2 \text{ PeV}$) of the cosmic ray spectrum given by Hillas (12).

Search Results :

1. Cygnus X-3 :

A search is made for evidence of continuous as well as pulsed UHE emission from this mysterious binary system which has been previously reported as a UHE gamma ray source. The database used in the present analysis was recorded between January 1993 and June 1994 with an effective on source observation time of 212.2 hours. The source is observed at NBU site at zenith angle 14° at the upper transit. Figure 3.18 shows the number of showers recorded in a declination

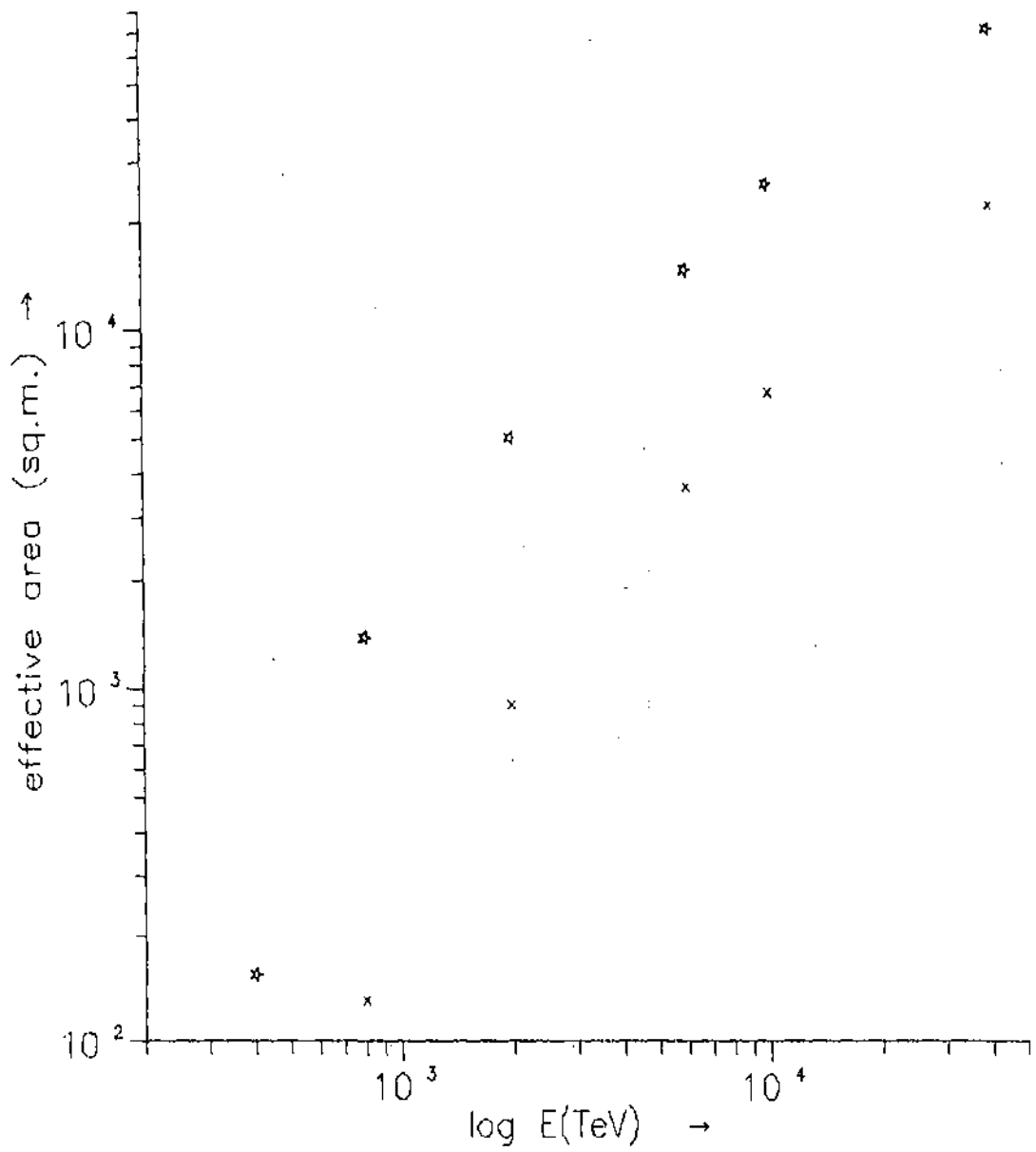


Fig 3.17 Effective area of the array as a function of primary gamma-ray energy. * - zenith angle 0°, x - zenith angle 30°.

band centered on Cygnus X-3 as a function of right ascension. The bins have 5^0 width in declination centered on 40.7^0 , the declination of Cygnus X-3. From the figure it is clear that there is a slight excess (1.79σ) of showers in the bin centered on the Cygnus X-3 for the full observing period. The total number of air showers observed in the source bin is 26 where the average background is only 18.33. The probability for a random excess of such magnitude is 1.89×10^{-2} . The time averaged integral flux for the excess is $F(>8 \times 10^{14} \text{ eV}) = (4.10 \pm 1.28) \times 10^{-13} \text{ cm}^{-2}\text{s}^{-1}$. The time averaged flux agrees well with the flux obtained in Akeho, MSU, Ooty observations (13,14,15).

The source events are then checked if they are co-related with the well known 4.8 hours periodic variation. For this purpose the arrival times of shower events from the position of Cygnus X-3 have been folded using an ephemeris by Van der Klis and Bonnet-Bidaud (18) observed from the X-ray data. Total phase is divided into 10 equal bins. Results are shown in fig 3.19. Concentrations of shower events are seen in the phase bin, .5-.6 in which 6 events are observed. The amount of excess is at 2.11σ level. The probability that 6 events might occur in any of the 10 phase bins at random out of a background of average value 2.6 per bin is 3.19×10^{-2} . The phase of emission is similar to the the present preferred UHE phase (phase $\sim .6$). However the statistical significance of these excesses are not high (within the 3σ limit) and a clearer picture will emerge only after analysis of more shower data.

2. Hercules X-1 :

There are several reports of continuous or sporadic UHE emission from Hercules X-1 as discussed in chapter one. NBU UHE database is looked for any evidence of continuous and pulsed emission from the direction of Hercules X-1. The effective on source observation time is 234.5 hours.

Figure 3.20 shows the number of EAS recorded as a function of right ascension in the declination band centered on Hercules X-1. The number of shower observed in the right ascension bin centered on Her X-1 is 28 where the average background is only 23. The poisson probability that this occurrence is due to chance 6.3×10^{-2} . The amount of excess (1.04σ) is well below the 3σ level. The time average integral flux corresponds to the excess of showers is $F(>8 \times 10^{14} \text{ eV}) = (2.42 \pm 1.08) \times 10^{-13} \text{ cm}^{-2}\text{s}^{-1}$.

Hercules X-1 is known to have an orbital period of 1.7 days. The detected events from the

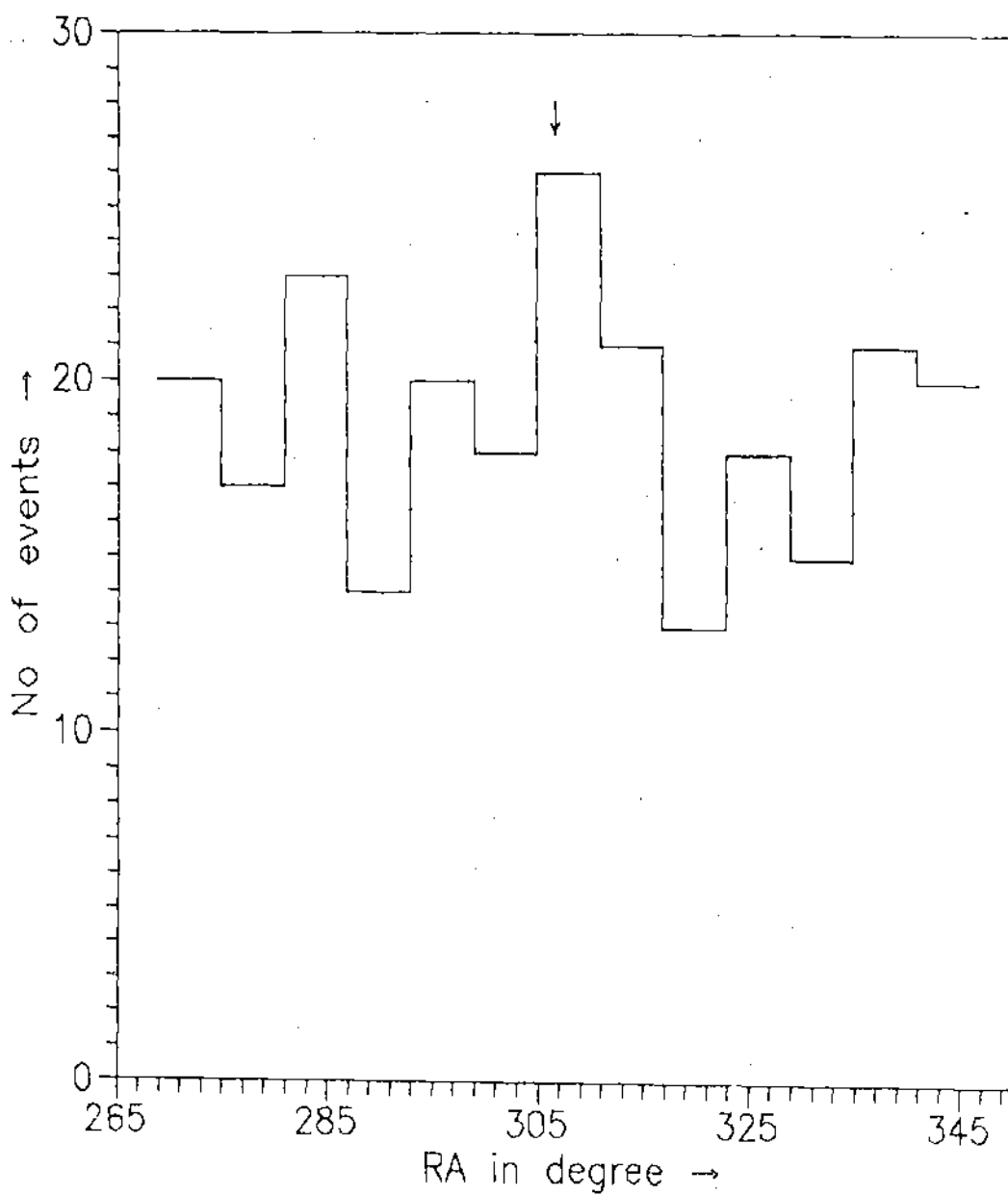


Fig 3.18 Number of observed EAS in the declination band centred on Cygnus X-3 as a function of right ascension.

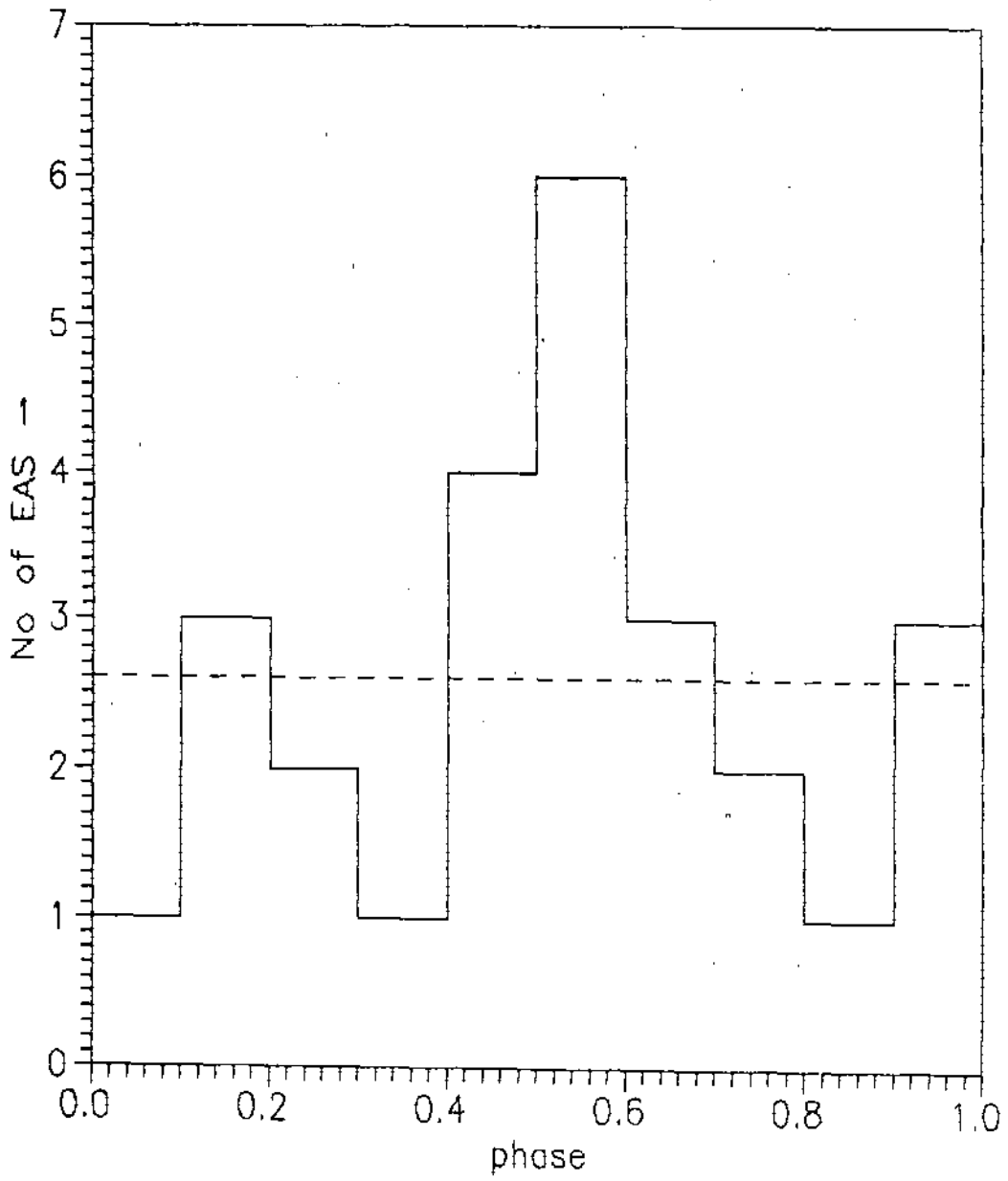


Fig 3.19 Orbital phase distribution of EAS from the direction of Cygnus X-3.

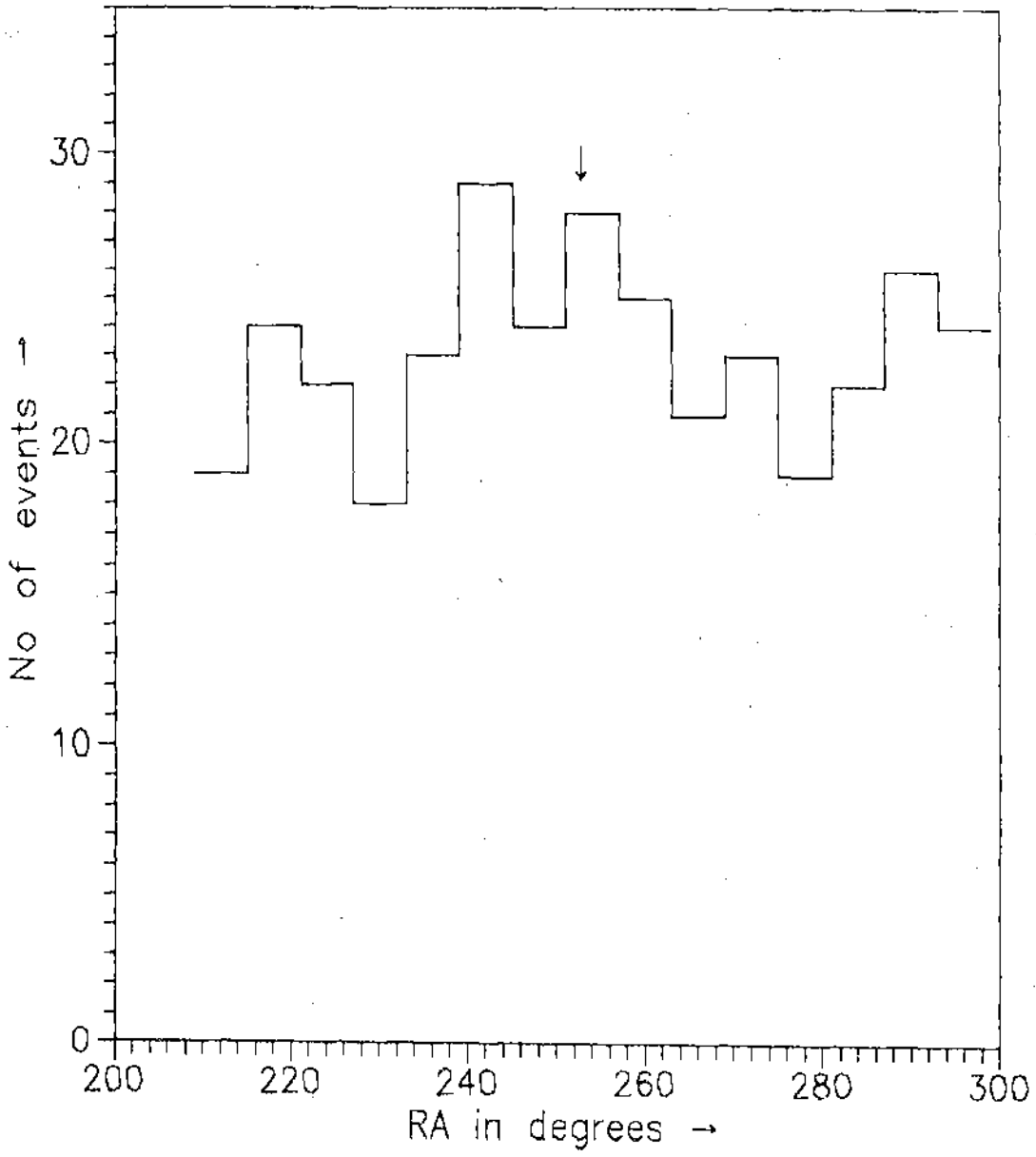


Fig 3.20 Number of observed EAS in the declination band centred on Hercules X-1 as a function of right ascension.

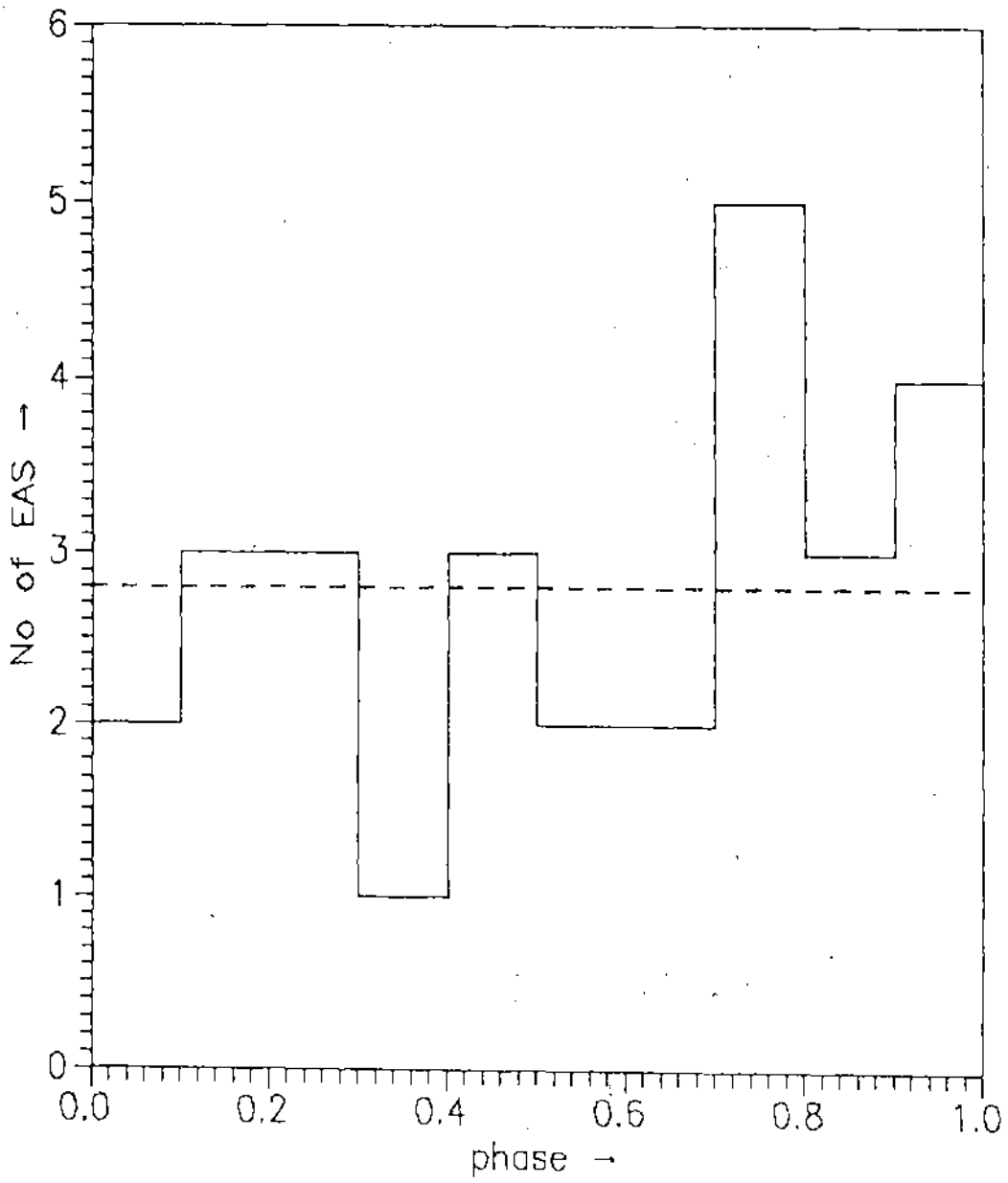


Fig 3.21 Phasogram of the events from the direction of Hercules X-1.

position of Her X-1 i.e, the on source events have been examined for coherence with the orbital period of 1.7 days. The Phasogram is shown in fig 3.21. The orbital period and the epoch are obtained from the ephemeris by Voges et al(19). No significant excess is found at any phase bin.

3. Crab-nebula :

We have searched for steady emission of UHE radiation from the region of Crab-nebula. The total effective observation time is 228.4 hours. Signal events are those falling within a source bin of width 5° in declination and 6° in right ascension. The number of events in the source bin is compared with the number of background events to search for evidence of emission. The results of this search are that 25 events is observed in the source bin against the average background of 25.05 events. The number of EAS events in the declination band centered on Crab-nebula as a function of right ascension is shown in fig 3.22. We found no evidence for UHE emission from the Crab-nebula.

4. Geminga :

Geminga is yet to be established a UHE potential gamma ray source though recently there are some positive reports for the detection of UHE radiation from the direction of Geminga. In the present analysis a search is made for steady emission of UHE radiation from the direction of Geminga. The right ascension distribution of events in the declination band centered on Geminga is shown in fig 3.23. The number of source events is 18 whereas the average value of the background is 17.92 . No evidence is seen for continuous emission in these data.

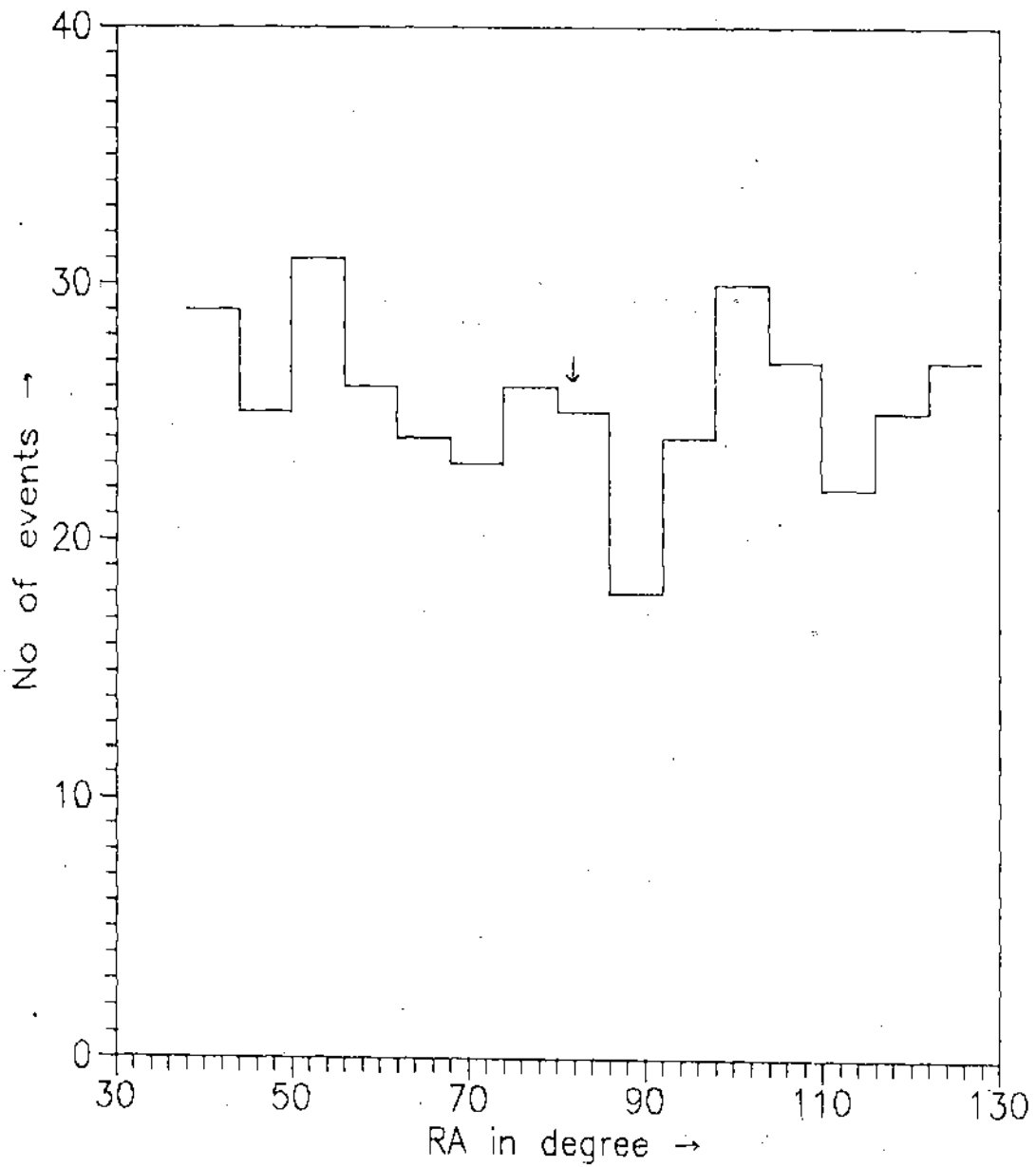


Fig 3.22 Number of observed EAS in the declination band centred on Crab Nabula as a function of right ascension.

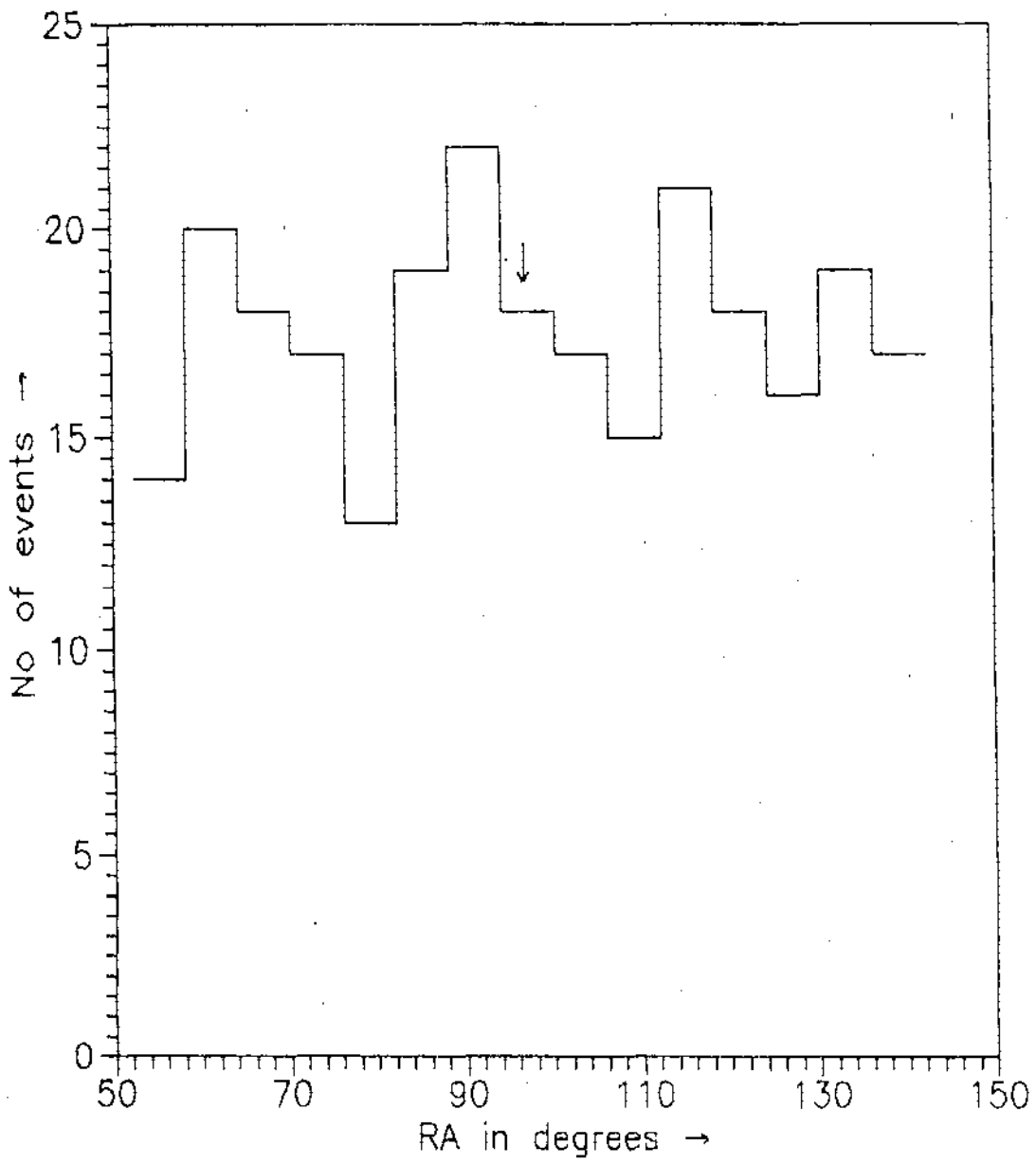


Fig 3.23 Number of observed EAS in the declination band centred on Geminga as a function of right ascension.